AIMS Geosciences, 8(2): 213–223.
DOI: 10.3934/geosci.2022012
Received: 04 December 2021
Revised: 12 January 2022
Accepted: 08 February 2022
Published: 23 February 2022

http://www.aimspress.com/journal/geosciences

Research article

Landscape mapping using ground-penetrating radar, electrical resistivity tomography survey and landscape profiling

Victor M Matasov[1,2,3], Svetlana S Bricheva[4,5,6,*], Alexey A Bobachev[7], Iya V Mironenko[2], Anton V Fedin[1,8], Vladislav V Sysuev[2], Lyudmila A Zolotaya[7] and Sergey B Roganov[2]

1. Department of Landscape Design and Sustainable Ecosystems, Agrarian-Technological Institute, Peoples' Friendship University of Russia—RUDN University, Moscow, Russia
2. Department of Physical Geography and Landscape Science, Faculty of Geography, Lomonosov MSU, Moscow, Russia
3. Faculty of Geography and Geoinformation Technology, Higher School of Economics, Moscow, Russia
4. Department of Seismic and Geoacoustic, Faculty of Geology, Lomonosov MSU, Moscow, Russia
5. Department of Quaternary paleogeography, Institute of Geography RAS, Moscow, Russia
6. Department of Geology and Geophysics NSU, Novosibirsk, Russia
7. Department of Geophysical Methods of Earth Crust Study, Faculty of Geology, Lomonosov MSU, Moscow, Russia
8. Laboratory of Geomorphology, Institute of Geography RAS, Moscow, Russia

* **Correspondence:** Email: bricheva@igras.ru; Tel: 79651129050.

Abstract: This work aims to verify and correct the boundary between two landscapes—moraine and outwash plain—delineated earlier by the classical landscape approach. The initial interpretation of the boundary caused controversy due to the appearance of the thermokarst depression in the outwash landscape. The lithological structure is one of the main factors of landscape differentiation. The classical approach includes drilling to obtain the lithological and sedimentary data. However, the boreholes are usually shallow, while geophysical methods allow to look deeper into the subsurface and improve our knowledge about lithological structure and stratigraphy. In this study, we use ground-penetrating radar with a peak frequency of 250 and 50 MHz and detailed electrical resistivity tomography (with 1 m electrode spacing) in addition to the landscape mapping and drilling to correct the landscape boundary position. We conclude that it is primarily defined by the subsurface

boundary between lithological complexes of clayish moraine deposits and sandy outwash deposits located at 7 m depth. Moving the boundary to the northeast by 70–100 m from the current position removes inconsistencies and clarifies the history of the area's formation in the Quaternary.

Keywords: critical zones; geophysical methods; landscape studies; Meshchyora lowlands

1. Introduction

Today the Earth's Critical Zone is an interdisciplinary research field that utilizes methods of physics, chemistry, geology, biology, climatology, and geography [1]. The term "critical zone" acquired its current meaning in the early 2000s [2]. It refers to the heterogeneous near-surface environment in which complex interactions between rocks, soils, water, air and living organisms regulate natural habitats and determine the availability of life-supporting resources. In Russian science, the term "landscape", known since the beginning of the 20th century, was developed to express the same idea [3]. The landscape is defined as a "genetically uniform territory, with regular and typical repetition of some interrelated combinations of geological structures, landforms, surface and groundwater, climate, soil types, phytocoenoses and zoocoenoses" [4]. Each landscape comprises different hierarchical morphological parts (levels of geosystems). The lithological structure is one of the leading components of the landscape, and its features influence vegetation cover, water behaviour, and ultimately human economic activity.

One of the most significant problems of Critical Zone Science is mapping the spatial distribution of different-scale land systems. The proper characterization and mapping of these systems have practical implications in landscape planning, forest cadastre and land valuation [5,6]. The classical approach, primarily based on a comprehensive description of relief, vegetation, soils and borehole data, have been actively complemented in recent decades by morphometric analysis of digital terrain models and remote sensing data [7,8].

Since the lithological structure is one of the main factors of landscape differentiation, the indication of geosystem boundaries (especially for a scale of landscape) should be based on lithological analysis. Applied geophysical methods such as ground-penetrating radar (GPR) and electrical resistivity tomography (ERT) are traditionally used for investigations in geomorphology and palaeogeography [9–11], geoarchaeology [12], soil science [13,14], ecology and forestry [15]. However, few works are devoted to their applications in Russian landscape studies [16,17].

This work aims to test the suitability of geophysical methods for defining the boundary between landscapes, observed earlier by the classical landscape approach, using the combination of GPR and ERT, supplemented by verification drilling.

2. Study area

The research was carried out at Lesunovo educational/research field station of the Faculty of Geography, Lomonosov Moscow State University, established in the 1970s to study the processes of landscape functioning and dynamics [18]. Lesunovo station is located in the southeast of the Meshchyora lowlands in the Ryazan region, on the boundary between moraine and outwash

landscapes. The Meshchyora lowlands is an area of modern slow tectonic subsidence situated at an absolute height of 90–150 meters; the crystalline basement is overlain by up to 60 meters of Quaternary deposits. The area relates to the Polessya type of landscapes, where thick layers of fluvioglacial deposits formed during the Dnieper-Moscow glacial epoch and underlain by moraine sediments of Don riverbed age prevail as a lithogenic base [18,19]. Widespread distribution of fluvioglacial sands creates favourable conditions for southern taiga pine forests. However, practically all forest communities (except floodplain communities) are at different stages of regeneration succession after fires and logging [19,20]. Mapping the local geosystem was performed in the 1970s using a 1 : 2000 scale topographic survey, aerial photography, a series of soil sampling and descriptions of sparse boreholes along with the palaeogeographical works [21,22]. Our investigation was conducted on a fallow field located west of Lesunovo village. As a result of the intense anthropogenic modification of the area due to farming activities, the geosystems are difficult to define based solely on visual observations. Thus, we investigated three roughly southwest-northeast oriented profiles across the suggested landscape boundary (Figure 1).

3. Materials and methods

We analysed the lateral landscape variation using landscape profiling, and vertical sedimentary structure interpreted from the GPR and ERT, constrained by borehole data. The results were combined to characterize and delimit the boundary between moraine and outwash landscapes.

3.1. Landscape profiling and drilling

We derived relief, soil and vegetation descriptions from the landscape map along the profile lines to constrain geophysical data. Moreover, soil samples were carried out along the profiles for every 25 meters to verify the current condition. Additionally, 5-meter depth boreholes were drilled using a manual hand auger (Royal Eijkelkamp, Netherlands) at some critical geosystems near the proposed landscape boundary. Sediment structure and moisture were described while drilling.

3.2. Ground-penetrating radar

GPR investigations were conducted in a profiling manner. We used two systems: bistatic impulse radar OKO-2 with 250 MHz antenna unit (Geotech, Russia); and monostatic radar Python-3 with 50 and 100 MHz antennas (Radar Systems, Inc., Latvia). Such a combination of frequencies allowed to get information to a depth of 8 m below the surface and compare the results with ERT data and borehole sediments. The resolution reaches nearly 15 cm for the 250 MHz antenna unit and 30–60 cm for 100 and 50 MHz. Profiles were processed using Prism2.7 and Radexplorer1.42 software with standard processing flow: automatic gain control, bandpass filtering, background removal and topographic correction. We used hyperbolic reflection patterns identified on many GPR profiles for electromagnetic waves' velocity determination. An average velocity was 10.8 cm/ns. Three profiles cut across the previously proposed landscape boundary (Figure 1). The total length of GPR profiles was 3000 m.

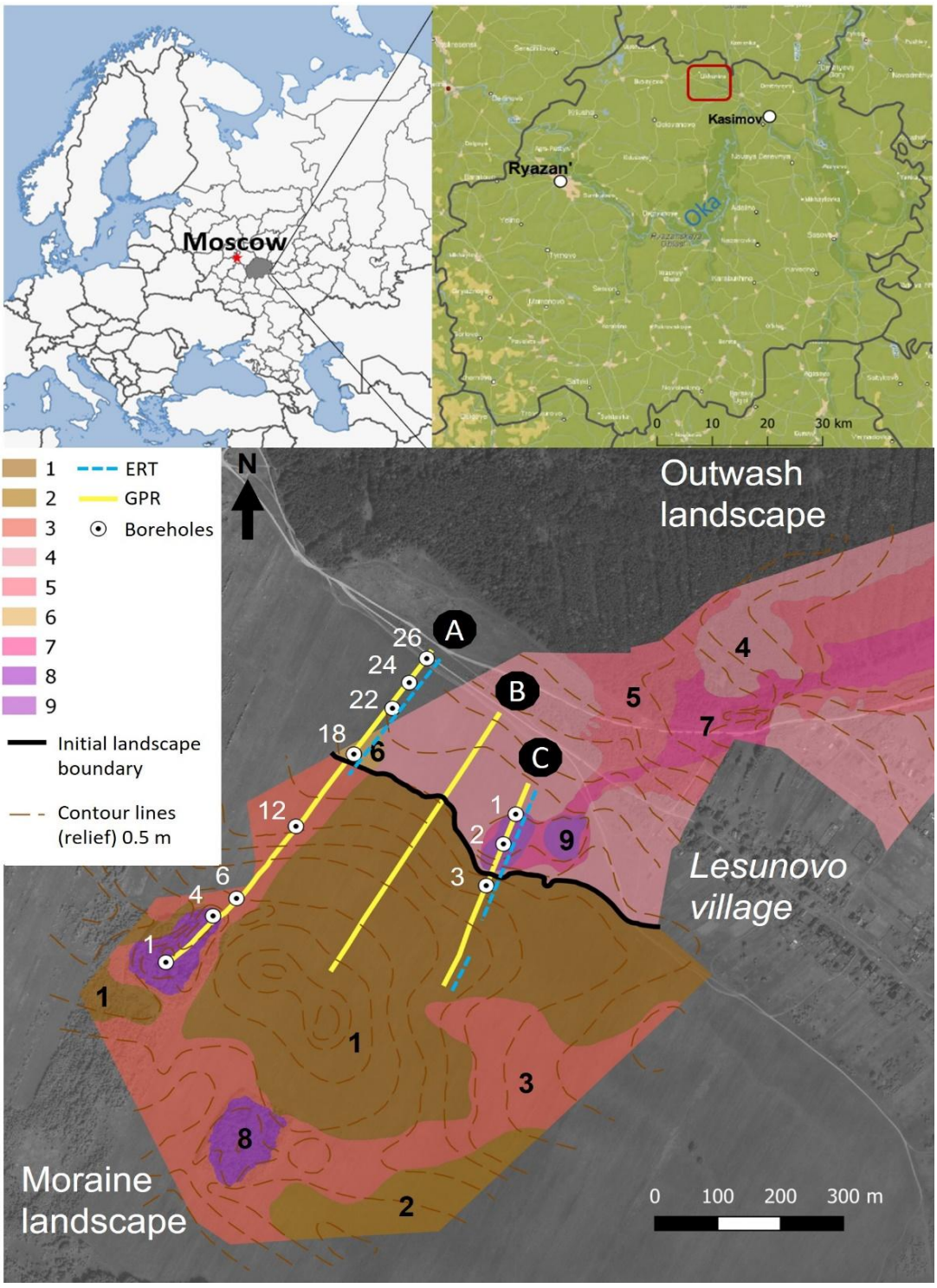

Figure 1. Study area at Lesunovo field station, Ryazan' oblast. The landscape map shows the main geosystem units 1–9 (modified from I.I. Mamai [22]): 1—Elevated parts of moraine plain; 2—Lower parts of moraine plain; 3—Ancient meltwater channels on moraine plain; 4—Elevated parts of outwash plain; 5—Mid-level parts of outwash plain; 6—Ancient meltwater channels on outwash plain; 7—Low-level parts of outwash plain; 8—Ancient thermokarst depression on moraine plain and 9—Ancient thermokarst depression on outwash plain.

3.3. Electrical resistivity tomography

ERT data were collected using a Syscal Pro Switch unit with 72 electrodes and 10 channels receiver (IRIS Instruments, France). Data were collected along lines A and C with 1 m electrode spacing. The relief was measured using a GNSS receiver. The total length of profiles is 531 meters. We used the following combination of arrays: forward and reversed Pole-Dipole array, Dipole-Dipole array (Figure 2). This combination is a suitable 2D inversion of ERT data [23]. The Pole-Dipole array has a sufficient spatial resolution and a high signal-to-noise ratio. On the other hand, Dipole-Dipole arrays are more sensitive to horizontal resistivity changes such as vertical and dipping structures while having a lower signal-to-noise ratio. The sensitivity of the Dipole-Dipole array is visible on pseudo-sections of apparent resistivity (Figure 2). Two-dimensional inversion of ERT profiles was done by RES2DINV software (Geotomo Software). The program produces a 2D resistivity model of the subsurface that best fits the measured resistivity values. The RMS error was less than 1 % for all profiles. The smoothness condition was used to increase the stability of the solution. This approach would lead to smooth solution resistivity transitions between different lithological blocks, even if contrasting boundaries appeared.

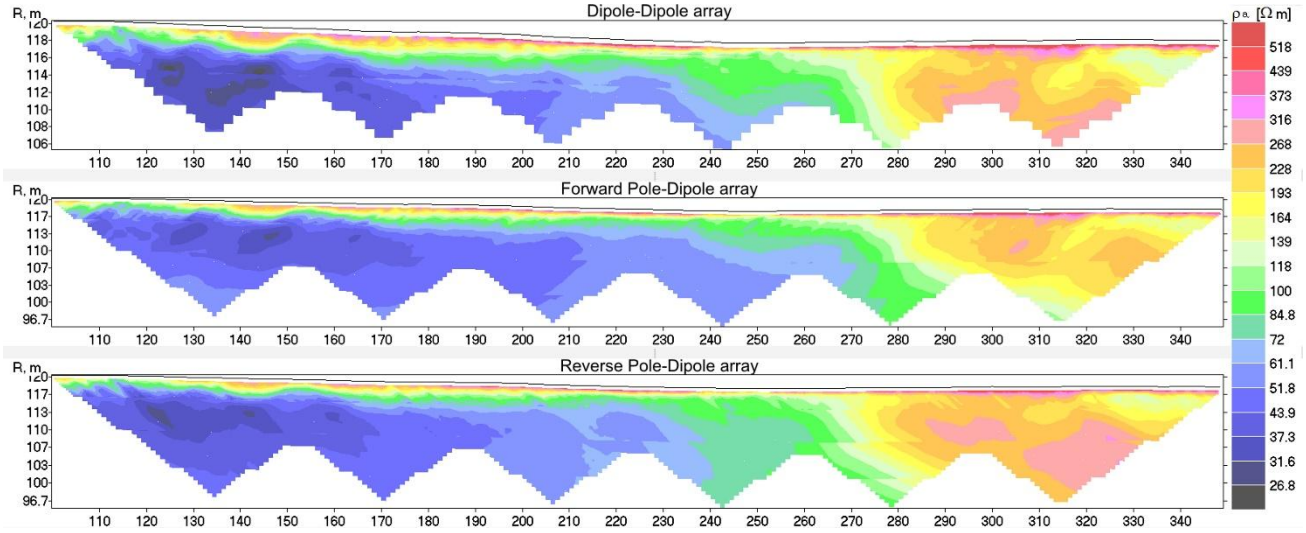

Figure 2. Apparent resistivity pseudo-sections with topography for line C (northeast end of the profile).

4. Results

Below we describe the GPR profiles with 250 and 50 MHz and the ERT inversion model obtained along line C, appropriately representing the main geomorphological features typical for the study area. According to the landscape map modified from I.I. Mamai [22], four geosystem units can be recognised on the profile in a southwest to the northeast direction (Figure 3A): the top of a moraine hill, gentle slope, thermokarst depression, outwash plain. These units correspond to the main geomorphologic features in the site, and subsequently, a good correlation between geophysical and borehole data allowed us to interpret the subsurface distribution of the mapped units.

4.1. The top of a moraine hill

In line C the moraine hill geomorphologic unit is located from 0 to 118 m (Figure 3A). This unit comprises the clayish moraine deposits covered with thin sandy loam layers based on borehole sediments from pits 6 and 12 in line A. The 250 MHz GPR profile shows that the moraine hill comprises a transparent wave pattern without bright reflections in the upper 1 m. At 1–2.5 m depth, a number of hyperbolae form a low-coherent reflection. Beneath it, the reflection amplitude decreases significantly. We trace this boundary on the first 230 m of the profile, although it loses contrast due to the deeper location to the northeast. The GPR data of lower frequency presents a similar pattern, generalised by reducing small-scale anomalies due to the lower resolution (Figure 3C). A significant part of the ERT profile along line C displays a low-resistivity zone ($\rho < 50$ Ohm*m) at a depth of 2 m, covered with sediments with resistivity values higher than 300 Ohm*m.

The upper part of the section could be interpreted as a thin (0–0.5 m) sand layer, underlined with clay-rich deposits. Diffraction hyperbolae are expected in the presence of cobble- and boulder-sized gravels common in moraine areas. The clayish moraine deposit controls the water table. They are significantly water-saturated thus we obtain the low-resistivity zone on the ERT profile. At the same time, the water content greatly influences the dielectric constant thus the GPR signal amplitude decreases on the top of the moraine. The GPR penetration depth together with resistivity values increase in the north-east, indicating the gradually exceeding percentage of the sand fraction over the clays.

4.2. Gentle slope

The slope is ploughed and overgrown with a fallow meadow; in line C it is located from 115 to 200 m (Figure 3A). Five lithological units were recognised in borehole C3. The uppermost unit 1 (0.3–1.9 m) comprises sandy deposits with loamy layers intercalations. It overlies loams of unit 2 (1.9–2.95 m) with a sharp boundary. Unit 3 (2.95–3.7 m) comprises wet silty sand. It is underlined with a thin (0.2 m) light loamy unit 4. The lowermost unit 5 (3.9–5 m depth) comprises a gravelly loam with clasts up to 1–2 cm in diameter. These deposits most likely correspond to fluvially reworked sediments from the morainic ridge.

The 250 MHz GPR data reveals the layered subsurface structure with a good resolution: the reflections at 2 and 3 m (Figure 3B) provide several GPR signatures, potentially corresponding to fluvially reworked packages. The low-frequency GPR image shows a regular subhorizontal reflection from the top of the moraine deposits located here at a depth of 3 m. The ERT profile suggests the same boundary at 3–3.5 m, represented as a low resistivity zone. The upper part of the ERT section is characterised by stratified resistivity distribution (300–700 Ohm*m). The geophysical results fit the borehole data and correspond to the change in grain size and moisture of sand and loam layers. Relatively high GPR signal amplitudes are potentially caused by the water table on the top of moraine. This, in turn, provides low resistivity values in the ERT section.

4.3. Thermokarst depression

This depression has a topographic expression, as seen in elliptical low in the map shown in Figure 1. Borehole C2 is filled with light sandy loam, underlaid with layers of sandy loams and sands. A bowl-shaped depression 1.5 to 2 m deep on the GPR profile is clearly distinguished between 230 and

270 m (Figure 3B). It is also presented on a 50 MHz profile; however, the pseudo-horizontal reflections with abrupt termination are observed at a depth of 5–6 m. The reason for strong difference in resistivity within the largely homogenous upper part of the section may be the increased moisture. The bottom of the depression, according to borehole data, is composed of loam, on which temporary waters can accumulate. The shape of the depression suggests its erosional origin. In the ERT profile, the depression is identified by an abrupt change in the resistivity of the top layer: its values decrease from 1000 Ohm*m to less than 300 Ohm*m. To the northeast from the depression, at 280 m, a sharp resistivity contrast is observed. We also mentioned its presence in the initial apparent resistivity pseudo-sections (Figure 2), and it stands out after inversion procedure. Estimating the dip angle from the ERT data is impossible, but a sub-vertical lithological boundary likely causes the resistivity contrast. High resistivity sediments predominate to the northeast of the border, while low resistivity sediments predominate to the southwest.

4.4. Outwash plain

The thickness of sandy deposits increases to the northeast part of the field as shown in borehole C1, which comprises sands up to 3.5 m. The electromagnetic signal penetration increases, and reflections up to 7 m depth can be detected in the 50 MHz data (Figure 3C). This package of reflections is subhorizontal and smooth. In comparison to the top of the moraine deposits, it has a lower amplitude and different frequency spectrum. The ERT data shows a layer with resistivity $\rho >$ 700 Ohm*m at depths of 10 m or more. Any of boreholes has not penetrated this layer. It is overlayed with a 3–4 m of deposits of low to medium resistivity values (ρ = 100–200 Ohm*m), representing laminated wet sands and loams.

5. Discussion

We propose that the boundary between moraine and outwash landscapes is primarily defined by the sub-vertical contact of clayish moraine deposits and sandy outwash deposits at a 7 m depth. This boundary is visible on ERT sections but is less evident on GPR profiles due to insufficient penetration depth. The proposed landscape boundary location is 70 m to the northeast from the first assumption based on the classical landscape approach. The GPR and ERT showed their worth in identifying lithologic units crucial for geosystems' delineating. The GPR wave patterns correlate with resistivity contrasts obtained from ERT and confirmed by borehole data.

Based on the data obtained in this study, supplemented by the maps of glaciations [24], we suggest the following geomorphological history of the area (Figure 3E). The moraine hill was formed by glacier activity during the Don glacial epoch (MIS 14). Later, the outwash plain was formed during the Moscow glaciation (MIS 6). In Valdai glacial epoch (MIS 5-MIS 2), this boundary was overlapped by aeolian and slope-wash deposits. The thermokarst depression is the youngest landform element embedded in the Late Glacial (late MIS 2) [25,26].

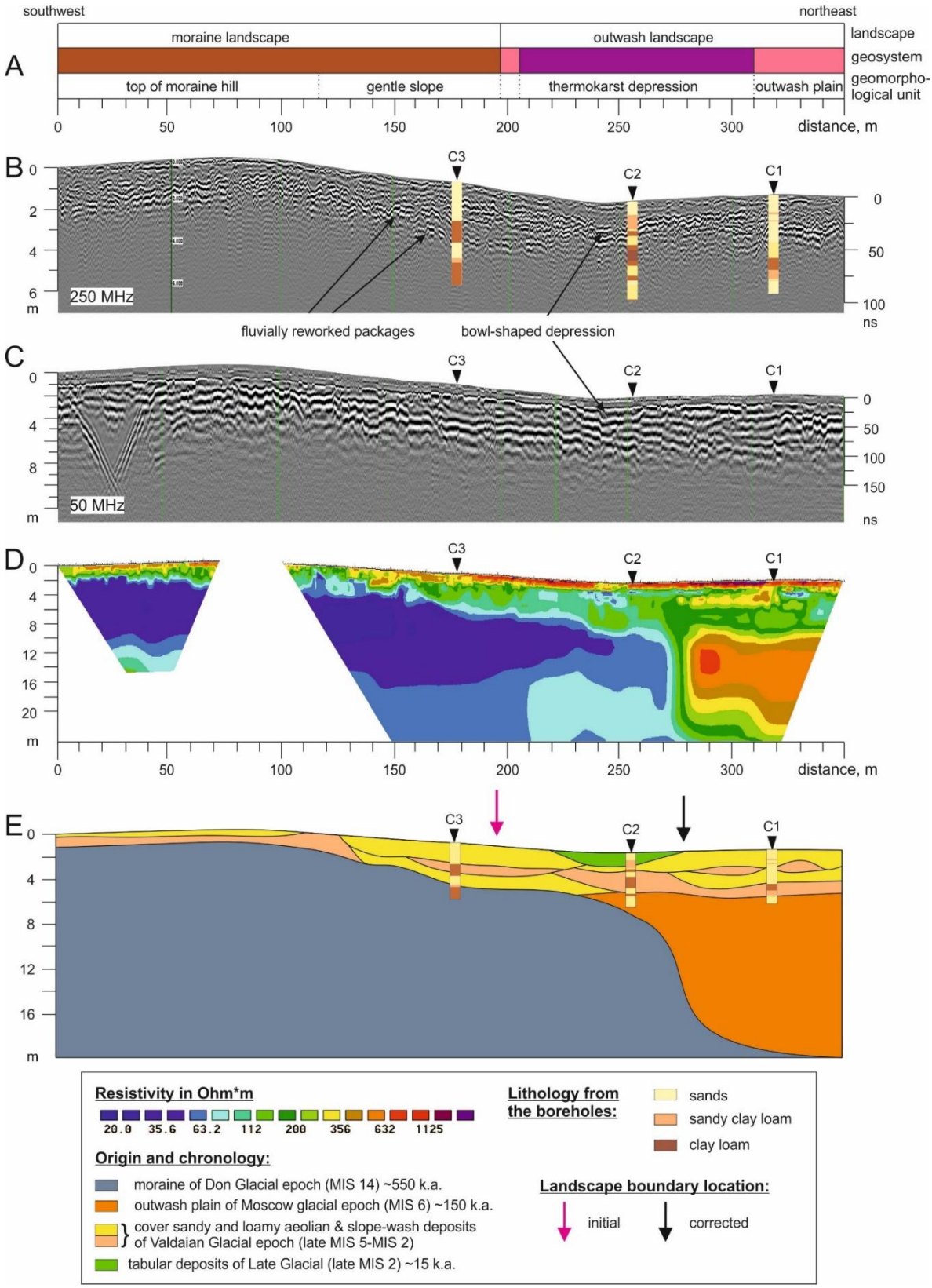

Figure 3. Survey results on line C: landscape and geomorphological units (A); GPR responses from 250 MHZ (B) and 50 MHz (C); ERT inversion (D) and integrated lithological section (E).

Moving the landscape boundary to the northeast by 70–100 m from the current position removes controversy due to the appearance of the thermokarst depressions in the outwash landscape. These depressions are more characteristic for the moraine landscape and are practically not found on the outwash plain. These results support modern palaeogeographical studies in that area and bring new data on sediments evolution to climate-vegetation reconstructions [19]. The intense land use of the area during the historical time (late XVI-XXI centuries) [20] results in modification of the vegetation and the first upper meter of the section. Thus, the geosystems' delineating based on visual observations becomes uncertain.

6. Conclusions

In landscape and Critical Zones studies, a detailed description of the shallow internal subsurface architecture is required. The classical landscape approach combined with near-surface geophysics clarifies the current landscape boundaries and the relationship between landscape components (soils, vegetation and sediments) and allows the proposal of integrated evolutional scenarios. The use of ground-penetrating radar and electrical resistivity tomography with 1 m electrode spacing makes it possible to reduce the resolution gap between the two methods and increase the overlapping zone of the respective datasets.

Acknowledgements

The budget funding of Lomonosov MSU supported the fieldwork. The data processing was carried out within the state assignment No. AAAA-A19-119021990091-4 (FMGE-2019-0005) of the Institute of Geography RAS. Furthermore we thank two anonymous reviewers and the editor Dr E. Vsemirnova for their suggestions to improve the quality of our manuscript.

Conflict of interest

All authors declare no conflicts of interest in this paper.

References

1. Fan B, Liu X, Zhu Q, et al. (2020) Exploring the interplay between infiltration dynamics and Critical Zone structures with multiscale geophysical imaging: A review. *Geoderma* 374: 114431. https://doi.org/10.1016/j.geoderma.2020.114431
2. Chorover J, Kretzschmar R, Garcia-Pichel F, et al. (2007) Soil Biogeochemical Processes within the Critical Zone. *Elements* 3: 321–326. https://doi.org/10.2113/gselements.3.5.321
3. Frolova M (2019) From the Russian/Soviet landscape concept to the geosystem approach to integrative environmental studies in an international context. *Landscape Ecol* 34: 1485–1502. https://doi.org/10.1007/s10980-018-0751-8
4. Solntsev NA (1948) The natural geographic landscape and some of its general rules. *Proc Second All-Union Geogr Congr* 1: 258–269.

5. Bryan BA (2003) Physical environmental modeling, visualization and query for supporting landscape planning decisions. *Landscape Urban Plann* 65: 237–259. https://doi.org/10.1016/S0169-2046(03)00059-8
6. Opdam P, Luque S, Nassauer J, et al. (2018) How can landscape ecology contribute to sustainability science? *Landscape Ecol* 33: 1–7. https://doi.org/10.1007/s10980-018-0610-7
7. Alekseeva NN, Klimanova OA, Khazieva ES (2017) Global land cover data bases and their perspectives for present-day landscapes mapping. *Izvestiya RAN Ser Geogr*, 110–123. https://doi.org/10.15356/0373-2444-2017-1-110-123
8. Lavalle C, Baranzelli C, Batista e Silva F, et al. (2011) A High Resolution Land Use/Cover Modelling Framework for Europe: Introducing the EU-ClueScanner100 Model, *Computational Science and Its Applications ICCSA 2011*, Berlin, Heidelberg, Springer, 60–75.
9. Bristow CS, Jol HM (2003) *Ground penetrating radar in sediments*, London, Geological Society. https://doi.org/10.1144/GSL.SP.2003.211
10. Bricheva SS, Modin IN, Panin AV, et al. (2020) The Structure of Quaternary Deposits in the Upper Dnieper Valley According to Integrated (Combined) Geophysical Data. *Moscow Univ Geol Bull* 75: 413–424. https://doi.org/10.3103/S014587522004002X
11. Pellicer XM, Gibson P (2011) Electrical resistivity and Ground Penetrating Radar for the characterisation of the internal architecture of Quaternary sediments in the Midlands of Ireland. *J Appl Geophys* 75: 638–647. https://doi.org/10.1016/j.jappgeo.2011.09.019
12. Conyers LB (2018) *Ground-penetrating Radar and Magnetometry for Buried Landscape Analysis*, Cham, Springer International Publishing.
13. Ryazantsev PA, Bakhmet ON (2020) Application of Geoelectric Methods for Mapping Soil Heterogeneity. *Eurasian Soil Sc* 53: 558–568. https://doi.org/10.1134/S1064229320050129
14. Zolotaya LA, Kosnyreva MV (2015) Ground-penetrating radar (GPR) researches in solving soil geophysics problems. *Geofizika* 2: 16–22.
15. Martin T, Nordsiek S, Weller A (2015) Low-Frequency Impedance Spectroscopy of Wood. *J Res Spectrosc* 2015: 9.
16. Bricheva SS, Matasov VM, Shilov PM (2017) Ground penetrating radar (GPR) as a part of integrated landscape studies on peatlands. *Geoecol Eng geol Hydrogeol Geocryology* 3: 76–83.
17. Sysuev VV (2014) Geo-radar investigation of the poly-scale structures in landscapes (case study of the Smolensk-Moscow highland). *Vestnik Mosk Univ Seriya 5 Geografiya* 4: 26–33.
18. Mamay II (1992) Dinamika landshaftov. Metodika izucheniya, Moskva, Izd-vo Mosk. un-ta. Available from: https://search.rsl.ru/ru/record/01001639692
19. Novenko EY, Tsyganov AN, Volkova EM, et al. (2016) Mid- and Late Holocene vegetation dynamics and fire history in the boreal forest of European Russia: A case study from Meshchera Lowlands. *Palaeogeogr Palaeoclimatol Palaeoecol* 459: 570–584. https://doi.org/10.1016/j.palaeo.2016.08.004
20. Matasov V, Prishchepov AV, Jepsen MR, et al. (2019) Spatial determinants and underlying drivers of land-use transitions in European Russia from 1770 to 2010. *J Land Use Sci* 14: 362–377. https://doi.org/10.1080/1747423X.2019.1709224
21. Aseev AA, Vedenskaya IE (1962) Razvitie rel'efa Meshcherskoj nizmennosti, Moskva, Izd-vo AN SSSR. Available from: https://search.rsl.ru/ru/record/01005950799

22. Mamay II (2013) Zakonomernosti projavlenija processov v landshaftah Meshhjory. Landshaftnyj sbornik (Razvitie idej N.A. Solnceva v sovremennom landshaftovedenii). M Smolensk: Ojkumena, 32–34. Available from: https://elibrary.ru/item.asp?id=25180335
23. Dahlin T, Zhou B (2004) A numerical comparison of 2D resistivity imaging with 10 electrode arrays. *Geophys Prospect* 52: 379–398. https://doi.org/10.1111/j.1365-2478.2004.00423.x
24. Astakhov V, Shkatova V, Zastrozhnov A, et al. (2016) Glaciomorphological Map of the Russian Federation. *Quat Int* 420: 4–14. https://doi.org/10.1016/j.quaint.2015.09.024
25. Kupriyanov DA, Novenko EY (2019) Reconstruction of the Holocene Dynamics of Forest Fires in the Central Part of Meshcherskaya Lowlands According to Antracological Analysis. *Contemp Probl Ecol* 12: 204–212. https://doi.org/10.1134/S1995425519030065
26. Novenko EY, Mironenko IV, Kupriyanov DA, et al. (2019) Pre-agrarian landscapes in Southeastern Meshchera: reconstruction from paleoecological data. *Geogr Nat Res*. Available from: https://elibrary.ru/item.asp?id=37418763&

AIMS Press